Practical evaluation of different modulation techniques for current-controlled voltage source inverters

J. Dixon
S. Tepper
L. Morán

Indexing terms: Modulation techniques, Current-controlled, voltage source inverter, Current-waveform, Simulation

Abstract: The quality of the current waveform generated by a current-controlled, voltage source inverter, depends basically on three factors: (a) the switching frequency of the PWM modulator; (b) the type of current waveform being generated; and (c) the modulation method used. In the paper, three modulation methods, whose characteristics are their simplicity, are analysed: periodical sampling control, hysteresis band control, and triangular carrier control. These three methods have been tested with three different waveform templates: sinusoidal, quasisquare and rectifier compensation current. They are compared in terms of the harmonic content and distortion at the same switching frequency. The paper shows that for sinusoidal current generation, the best method is the triangular carrier, followed by the hysteresis band and the periodical sampling. However, for the other two types of reference templates, the analysis showed that, depending on external factors such as inverter inductance, type of load, or delays in the PWM switching signals, one strategy may be better than the others. The paper shows that each control method is affected in a different way by the switching time delays present in the driving circuitry and in the power semiconductors. The results are analysed and compared, with the help of computer simulations and experimental results.

1 Introduction

Current source converters play an important role in the control of alternating current machines, special power rectifiers and active power filters [1–3]. One of the most popular current source inverters is the current-controlled voltage source inverter (CCVSI), shown in Fig. 1. The CCVSI allows an easy control of power in the four quadrants, with current reversal at a fixed power factor. Some applications need sinusoidal current waveforms (induction and synchronous machines, power factor compensators and bidirectional rectifiers). Some others need trapezoidal or quasisquare current waveforms, like brushless dc permanent magnet machines. On the other hand, shunt active power filters need a variety of current waveforms to compensate different harmonic currents in a nonlinear load. A typical current active filter's need to compensate could be the harmonic content generated by a full-wave three-phase rectifier, which will be called compensation current for six-pulse rectifier (RCCW). This work analyses the waveform quality of the current generated using three different current waveform templates and three different modulation methods. The three templates analysed are: (i) sinusoidal current waveform (SCW); (ii) quasisquare current waveform (QSCW); and (iii) compensation current for six-pulse rectifier (RCCW). The modulation methods used to test the quality of the current for the three waveforms aforementioned are: (a) the periodical sampling method (PS); (b) the hysteresis band method (HB); and (c) the triangular carrier method, which are characterised for their simplicity. These three modulation methods are shown in Figs. 2–4 and are explained briefly later. Previous work [4–8] has shown partial results related to harmonic distortion and modulation methods but none of them makes an analysis comparison of the results obtained.

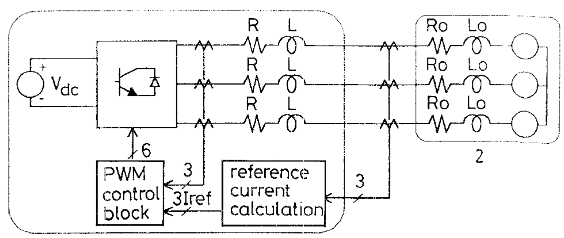

Fig. 1 *Block diagram of the CCVSI*
1 current-controlled voltage source inverter; 2 load

IEE Proceedings online no. 19960411

Paper first received 21st August 1995 and in revised form 19th February 1996

J. Dixon and S. Tepper are with the Department of Electrical Engineering, Pontificia Universidad Católica de Chile, Casilla 306, Correo 22, Santiago, Chile

L. Morán is with the Department of Electrical Engineering, Universidad de Concepción, Casilla 53–C, Concepción, Chile

2 Analysis of the PWM generators

2.1 Description of the modulation methods

In this paper three different methods of modulation are analysed: periodical sampling (PS), hysteresis band (HB), and triangular carrier (TC).

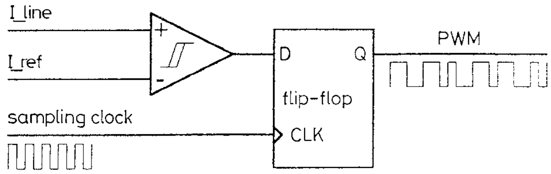

Fig. 2 *Modulation control block: periodical sampling (PS)*

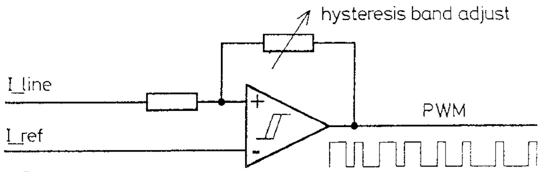

Fig. 3 *Modulation control block: hysteresis band (HB)*

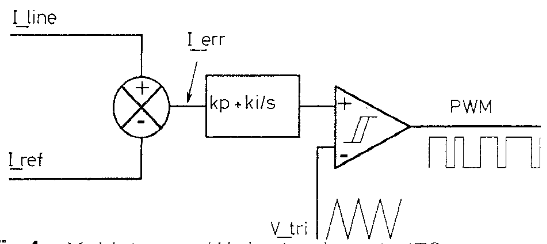

Fig. 4 *Modulation control block: triangular carrier (TC)*

The PS method switches the power transistors of the active filter during the transitions of a squarewave clock of fixed frequency: the sampling frequency. As shown in Fig. 2, this type of control is very simple to implement: only a comparator and a D-type flip-flop are needed per phase. The main advantage of this method is that the minimum time between switching transitions is limited to the period of the sampling clock [6]. However, the actual switching frequency is not clearly defined.

The HB method switches the transistors when the error exceeds a fixed magnitude: the hysteresis band. As can be seen in Fig. 3, this type of control needs a single comparator with hysteresis per phase. In this case the switching frequency is not determined, but it can be estimated from [7].

The TC method, shown in Fig. 4, compares the output current error with a fixed amplitude and frequency triangular wave: the triangular carrier. The error is processed through a proportional-integral (PI) gain stage before the comparison with the triangular carrier takes place. As can be seen, this control scheme is more complex than PS and HB. The values for kp and ki determine the transient response and steady state error of the TC method [8]. It was found empirically that the values for kp and ki shown in Eqns. 1 and 2 give a good dynamic performance under several operating conditions:

$$kp^* = \frac{(L + Lo) \cdot \omega_c}{2 \cdot V_{dc}} \tag{1}$$

$$ki^* = \omega_c \cdot kp^* \tag{2}$$

where $L+Lo$ is the total series inductance seen by the CCVSI, ω_c is the triangular carrier frequency, whose amplitude is 1V p-p, and V_{dc} is the DC supply voltage of the inverter.

2.2 Reference waveforms under study

The control methods are tested with three different waveforms: (i) sinusoidal current waveform (SCW); (ii) quasisquare current waveform (QSCW); and (iii) six-pulse rectifier compensating current waveform (RCCW). Fig. 5 shows these waveforms for a 50Hz fundamental frequency. Because the CCVSI cannot generate an infinite slope current (di/dt), the maximum slope of the waveforms are limited to the maximum di/dt imposed by the total series inductance ($L + Lo$). This permits a better comparison of the control methods.

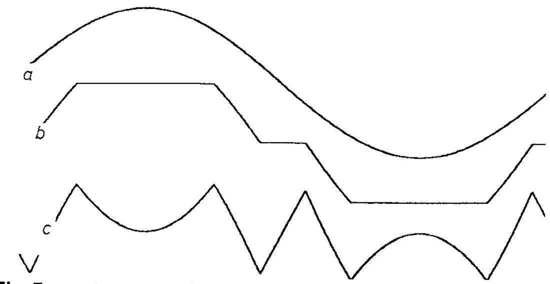

Fig. 5 *Reference waveforms*
a Sinusoidal current waveform (SCW)
b Quasisquare current waveform (QSCW)
c Compensation current for six-pulse rectifier (RCCW)

The SCW is used in power factor correction and machine drives. In the experiments and simulations a 10A peak reference current was used. The choice of this value is related with the maximum di/dt imposed by the total series inductance ($L + Lo$ = 13mH), which only permits a maximum of 20A peak reference. Approaching this limit value, the three methods give similar results, and above this value, the currents cannot follow the references. Then, 10A represents 50% of the maximum allowable current, and permits one to see a clear difference between the three modulation methods.

The QSCW finds application in driving brushless DC motors. Due to its stepped shape this waveform is well suited for comparing the transient response of the different control methods. A 10A peak QSCW was used for the experiments and simulations, corresponding to an effective output current near to 7.87A.

The RCCW is a typical current waveform for an active filter feeding a six-pulse rectifier load. This waveform contains only harmonics of the fundamental, but not the fundamental itself. In the experiments and simulations a 5A peak RCCW was used, corresponding to an effective output current near to 2.51A.

2.3 Comparison of the control methods

The control methods are compared at the same switching frequency to ensure similar losses and similar speed switching devices. This permits a direct comparison on how efficient, in terms of low distortion, these control methods are.

In order to measure the level of distortion (or undesired harmonic generation) introduced by the control methods under study, eqn. 3 is defined:

$$\%\text{Distortion} = \frac{100}{I_{\text{rms}}} \sqrt{\frac{1}{T} \cdot \int_T \cdot (i_{\text{line}} - i_{\text{ref}})^2 \, dt} \tag{3}$$

where the term I_{rms} is the effective value of the desired current. The term inside the square root gives the RMS value of the error current, which is undesired. This formula measures the percentage error (or distortion) of the generated waveform. This definition is independent of the reference waveform, being a good choice for comparing the performance of the CCVSI. It should be noticed also that this definition considers the ripple, amplitude and phase errors of the measured waveform, as opposed to THD, which does not take into account offsets, scaling and phase shifts.

3 Power converter simulations

The simulations are based on the CCVSI and load presented in Fig. 1. The AC mains is not considered in the simulations.

3.1 Simulations with sinusoidal current waveforms

The DC voltage V_{dc} was set to 150V. The value of $R + Ro$ was 2ohms, and $L + Lo$ was 13mH.

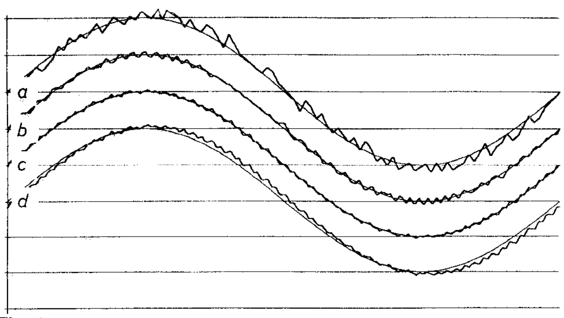

Fig. 6 *Waveforms obtained using 1.5kHz switching frequency and L + Lo = 13mH*
(a) PS method, (b) HB method,
(c) TC method ($kp^* + ki^*$), (d) TC method (kp^* only)
Vertical scale 5A/div

Fig. 6 shows the current waveforms generated by the control methods for a switching frequency of 1.5kHz. It can be seen that for PS control, the generated current does not swing symmetrically around the reference: it has a biasing error. In HB the generated current oscillates symmetrically around the reference with the consequent smaller distortion than PS. The current waveform generated by TC with PI gain (TC–PI) is similar to HB but with lower ripple. The TC method with proportional gain (TC–P) has also low ripple, but it has an amplitude and phase error that gives a higher percentage distortion. (It should be kept in mind that the distortion measure given by eqn. 3 considers not only the ripple, but also the amplitude and phase errors.)

In Fig. 7 the methods under study are compared in terms of distortion versus switching frequency, using a sinusoidal waveform reference. It can be seen that TC–PI is the best, followed by HB and TC–P. The worst method is PS.

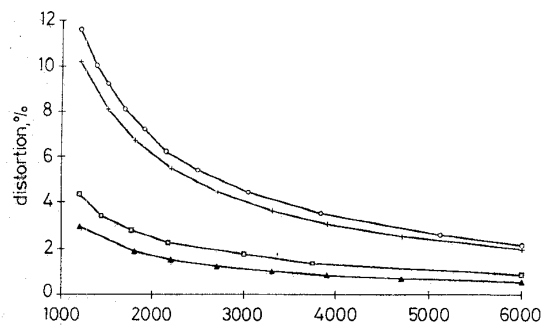

Fig. 7 *Distortion comparison for sinusoidal reference*
∘ PS; □ HB; ▲ TC ($kp^* + ki^*$); + TC (kp^* only)

In Figs. 8–10, the frequency spectra generated for a switching frequency of 1.5kHz are shown. In order to obtain the same switching frequency in the three methods, the sampling frequency was set to 3500Hz for PS, the hysteresis band was set to 0.56A for HB, and the triangular carrier was adjusted to 1500Hz for TC–PI. As it can be seen that the spectrum of PS is not clearly related to the switching frequency and contains odd and even harmonics, however, it is interesting to notice a minimum around the harmonic #70, which corresponds to the 3500Hz sampling frequency. The spectrum of HB resembles that of PS, but the harmonics are of lower magnitude. Finally, the spectrum of the TC–PI method is concentrated in sidebands around harmonics 20, 40, 60, etc., which correspond to the triangular carrier frequency harmonics. As can be seen, TC–PI is very useful where a single fixed frequency is to be produced, because the harmonics are well defined and can be eliminated with small passive filters.

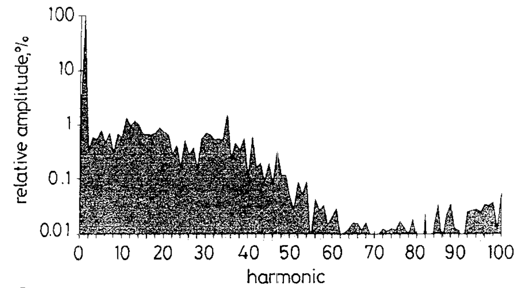

Fig. 8 *Frequency spectra comparison for SCW, using 1.5kHz switching frequency: PS*

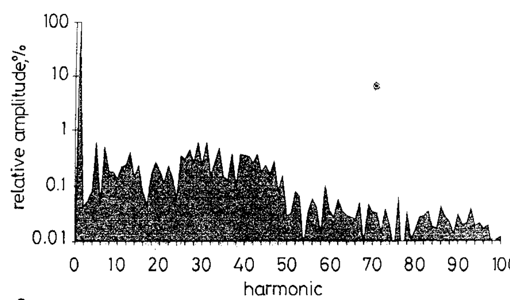

Fig. 9 *Frequency spectra comparison for SCW, using 1.5kHz switching frequency: HB*

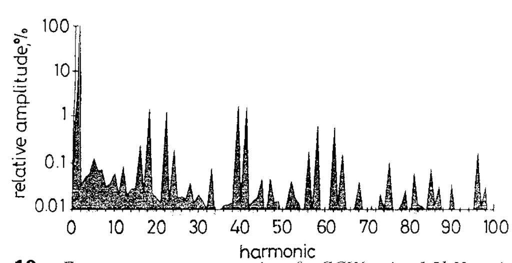

Fig. 10 *Frequency spectra comparison for SCW, using 1.5kHz switching frequency: TC*

3.2 Simulations with quasisquare current waveforms

Fig. 11 shows the waveforms generated with the three control methods using a switching frequency of 2kHz. As can be seen, the output current cannot follow the slope of the reference. Under this condition, the HB method seems to be the best, followed by TC–P and PS. On the other hand, TC–PI is strongly affected by the failure to follow the reference because the error accumulates in the integrator and finally produces an overshoot. It should be noticed that the integral gain for this case was reduced from ki^* to $0.1ki^*$, because the former value caused instability in the output current.

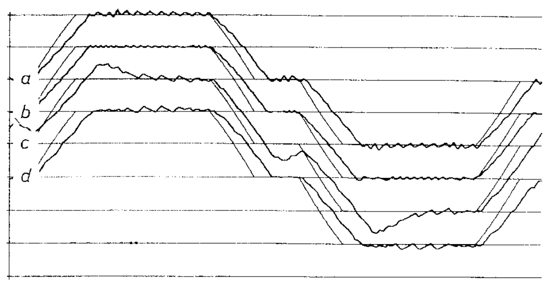

Fig. 11 *Waveforms obtained with 2kHz switching frequency and L + Lo = 13mH*
a PS method, *b* HB method, *c* TC method ($kp^* + ki^*$), *d* TC method (kp^* only)
Vertical scale 5 A/div

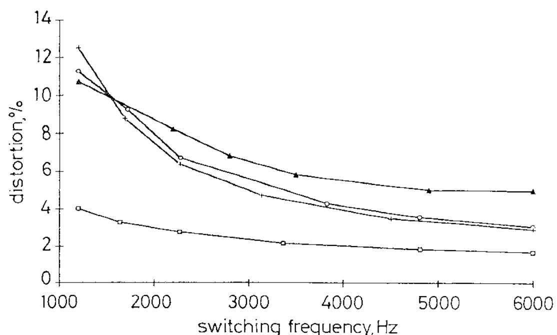

Fig. 12 *Distortion comparison for QSCW reference with L + L0 = 13mH*
◦ PS; □ HB; ▲ TC ($kp^* + 0.25ki^*$); + TC (kp^* only)

Fig. 12 shows the distortion of the waveforms of Fig. 11. As it can be seen that the TC–P and TC–PI methods are the worst. In the case of TC–P, the generated current has a permanent error due to a scaling factor. In the TC–PI case the error source is the overshoot. It can be seen that the HB method is the best under these conditions.

In order to make a fair comparison for the TC method, the value of $L + Lo$ was lowered from 13 to 5mH so that the currents generated by the inverter could follow the slope of the reference current. As can be seen in Fig. 13, under this condition the TC–PI method works well. In Fig. 14 the percentage distortion generated by the three methods at different switching frequencies is shown. In this case the best method is TC, closely followed by HB, with PS in third place. As can be seen, it is important for the TC–PI method that it can follow the slope of the reference at all times, otherwise it may be subject to overshoots.

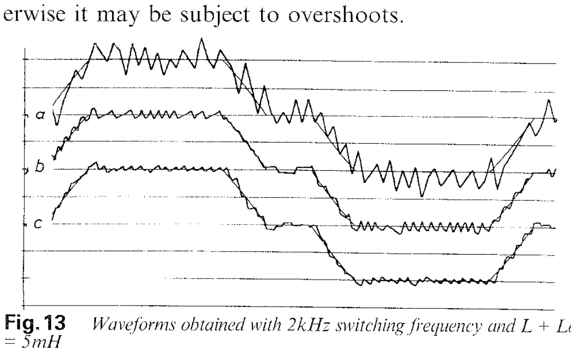

Fig. 13 *Waveforms obtained with 2kHz switching frequency and L + Lo = 5mH*
a PS method, *b* HB method, *c* TC method ($kp^* + ki^*$)

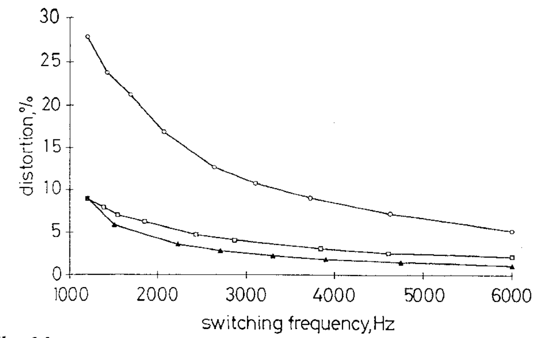

Fig. 14 *Distortion comparison for QSCW reference with L + Lo = 5mH*
◦ PS; □ HB; ▲ TC ($kp^* + ki^*$)

3.3 Simulations with rectifier compensation current

In Fig. 15, the waveforms obtained for a RCCW reference at 2kHz switching frequency and $L + Lo$ = 5mH are shown. In this case the HB method and TC–PI method are similar, and PS is clearly the worst. Fig. 16 shows the percentage distortion at different frequencies for the three methods. In this case HB and TC–PI are quite similar for frequencies above 2.8kHz, but for lower frequencies HB seems to be better because of its better transient response. The PS method again is the worst.

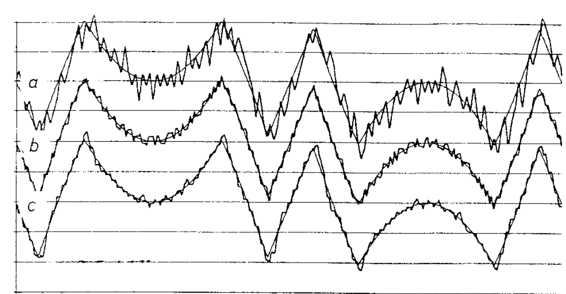

Fig. 15 *Waveforms obtained with 2kHz switching frequency and L + Lo = 5mH*
a PS method, *b* HB method, *c* TC method ($kp^* + ki^*$)

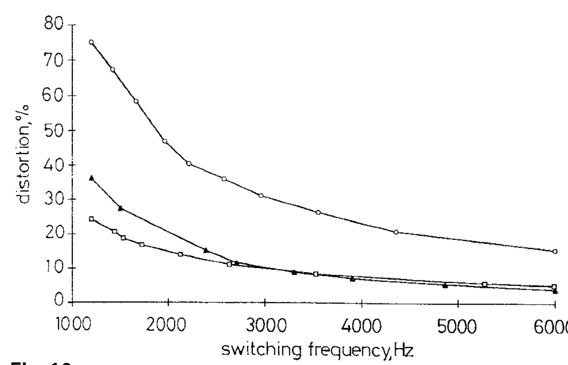

Fig. 16 *Distortion comparison for RCCW reference with L + Lo = 5mH*
◦ PS; □ HB; ▲ TC ($kp^* + ki$)

3.4 Switching time delay effects

The earlier simulations did not take into account time delays present in the driver circuits, and turn-on and turn-off times of the power semiconductors. For instance, an optocoupled driver has a typical delay of 10μs. Adding to the driver delay, a power transistor can have a total turn-off time ranging from a few microseconds for medium power MOSFETs to as long as 100μs for very high current bipolar devices.

To illustrate the effect of the delays associated with the inverter, a representative total delay of 40μs was considered. Figs. 17, 18 and 19 compare the performance of the PS, HB and TC–PI methods, respectively, for a sinusoidal current reference and different switching frequencies. In this case the series inductance $L + Lo$ was 13mH.

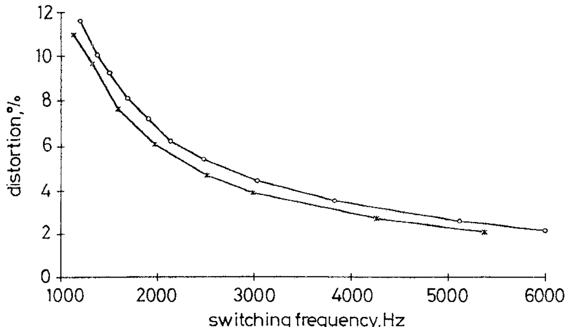

Fig. 17 *Distortion comparison of PS with 40μs switching delay*
(×) *with ideal PS* (○)

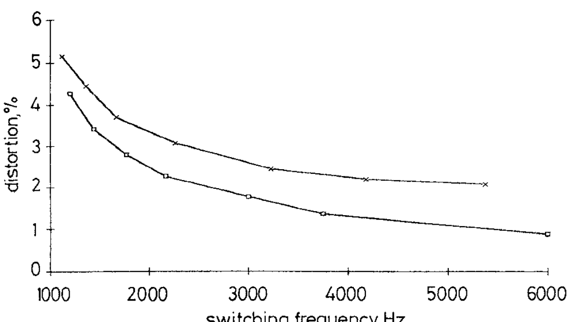

Fig. 18 *Distortion comparison of HB with 40μs switching delay*
(×) *with ideal HB* (□)

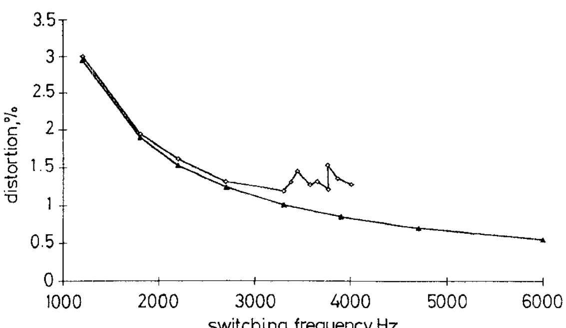

Fig. 19 *Distortion comparison of TC with 40μs switching delay*
(◊) *with ideal TC* (▲)

As shown in Fig. 17, PS seems to benefit from moderate time delays. This is explained by the fact that a time delay makes the current swing around the reference, instead of being above it or below it most of the time (as could be seen in Fig. 6 trace (a)). In the case of HB, the hysteresis band limit is violated when switching delays are present. In order to keep the frequency constant (with respect to the case without delays) this band was made smaller until the same switching frequency was obtained. Under these circumstances, the HB method shows higher distortion than the ideal case, as shown in Fig. 18. This is because the delays make the current swing unsymmetrically around the band, thus generating an offset error similar to the PS method in Fig. 4 trace (a). Finally the TC–PI method is clearly affected by the 40μs delay, as shown in Fig. 19. It is interesting to notice that at frequencies above 3.3kHz the current control loop becomes unstable because the stability margin has been reduced by the added delay.

4 Experimental results

The experimental results were taken in a 2kVA current-controlled voltage source inverter, similar to the drawing shown in Fig. 1. The DC supply was 150V, the total series inductance $L + Lo$ was 13mH, the total series resistance $R + Ro$ was 2ohms, and the time delays associated with the driving circuitry and transistor turn-off delays were about 40μs.

In Figs. 20, 21 and 22, real current waveforms obtained from the three control methods are shown (periodic sampling, hysteresis band and triangular carrier).

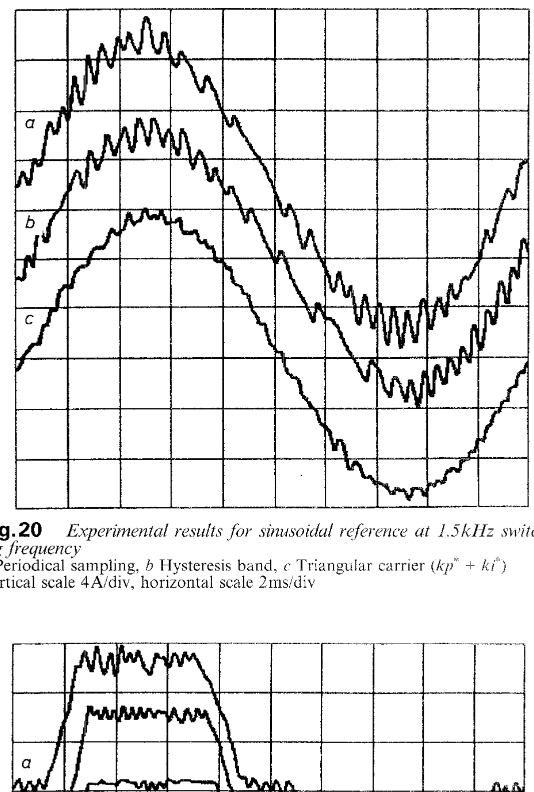

Fig. 20 *Experimental results for sinusoidal reference at 1.5kHz switching frequency*
a Periodical sampling, *b* Hysteresis band, *c* Triangular carrier ($kp^* + ki^*$)
Vertical scale 4A/div, horizontal scale 2ms/div

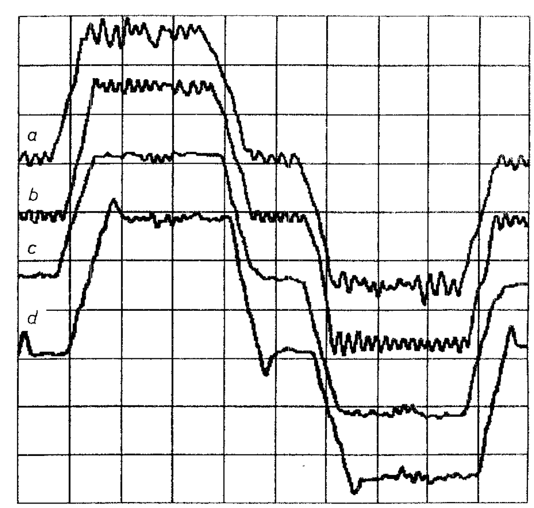

Fig. 21 *Experimental results for quasisquare current reference at 2kHz switching frequency*
a Periodical sampling, *b* Hysteresis band, *c* Triangular carrier (kp^* only), *d* Triangular carrier ($kp^* + 0.1ki^*$)
Vertical scale 4 A/div, horizontal scale 2 ms/div

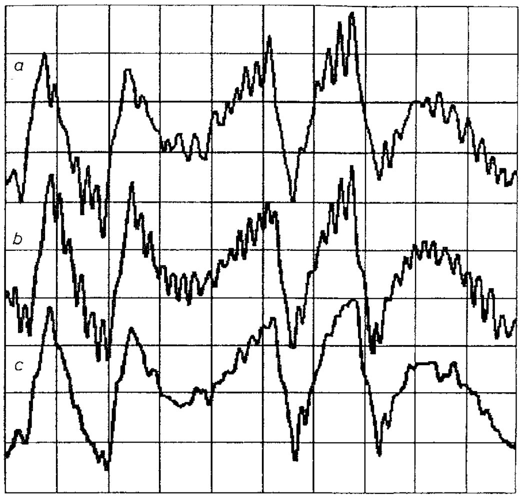

Fig. 22 *Experimental results for six-pulse rectifier compensating current at 2kHz switching frequency*
a Periodical sampling, *b* Hysteresis band, *c* Triangular carrier (kp^* only)
Vertical scale 2.5A/div, horizontal scale 2ms/div

Fig. 20 shows the waveforms obtained with sinusoidal reference using a switching frequency of 1.5kHz. For this case the TC–PI method is the best, followed by HB and PS.

Fig. 21 shows the waveforms obtained with a quasisquare current reference using a switching frequency of 2kHz. Although it is not clear in this oscillogram, the HB method is better than TC–P in terms of the distortion measure used in this work. On the other hand, TC–PI with $kp^* + 0.25ki^*$ has some overshoots, but the ripple is lower than HB. Finally, PS is clearly the worst.

Fig. 22 shows the waveforms obtained with a six-pulse rectifier compensating current reference, using a switching frequency of 2kHz. In this case, HB gives less distortion than PS, and TC becomes the worst because it introduces a small phase shift between the reference and the real current. In the case where real switching time delays exist, PS should be improved while HB and TC–PI should be degraded with respect to the waveforms shown in Fig. 14. The time delay where PS becomes better than HB will depend on the parameters of the converter. In the particular case of the converter used in the experiments, this value is around 60μs. It is important to mention that PS has some advantages over the HB, such as a defined switching frequency and simpler microcomputer control, because sampling is generated by the clock. The waveforms in Fig. 14 were taken with $L + Lo = 5$mH, while the experimental results in Fig. 22 used $L + Lo = 13$mH. However, this does not affect the validity of the previous statement.

5 Conclusions

Three different methods of current modulation to control current-controlled voltage source inverters (CCVSI), have been implemented and evaluated, using three different current reference waveforms: sinusoidal (SCW), quasisquare (QSCW), and rectifier compensating current (RCCW). The methods of modulation used to follow these references were: periodical sampling (PS), hysteresis band (HB) and triangular carrier (TC).

From the results obtained, and based on the particular conditions in which the simulations and experiments were performed, the following can be concluded:

(1) In sinusoidal current generation the best method is TC–PI because the harmonic distortion and the current ripple are lower than with the other methods. It is interesting to notice that the harmonic spectrum is related to the triangular carrier frequency, so it can be attenuated in some cases by resonant passive filters.

(2) In applications that must generate stepping currents and high-order harmonics the HB method is the best because of its excellent transient response, followed by TC with proportional gain, because of the low ripple and distortion. If the compensating current is required to have precise amplitude and phase, the best method is HB because TC with proportional gain has a permanent error in the output current. In most cases the reference current may have steps that cannot be followed immediately by the active filter. In these cases the TC method with proportional-integral gain is not recommended because it presents overshoot problems.

(3) From the simulations it can be stated that the periodical sampling method improves with moderate time delays and the hysteresis band method deteriorates. It is possible to think that when very slow power switches are used the PS method could perform better than the HB method. However, further investigation has to be performed to ensure the validity of this last statement. On the other hand, the triangular carrier method with PI gain is seriously affected by time delays because the stability margin is reduced and current control may become unstable.

6 Acknowledgments

The authors thank the 'Fondo de Desarrollo Científico y Tecnológico', FONDECYT, through project numbers 997–94 and 652–93, for the financial support which made it possible to do this research.

7 References

1 BROD, D., and NOVOTNY, D.: 'Current control of VSI-PWM inverters', *IEEE Trans.*, 1985, **IA-21**, (4), pp. 562–570
2 MALESANI, L., ROSSETTO, L., and TENTI, P.: 'Active filters for reactive power and harmonic compensation'. *Proceedings of the IEEE-PESC*, June 1986, pp. 321–330
3 MORÁN, L., MORA, E., WALLACE, R., and DIXON, J.: 'Performance analysis of a power factor compensator which simultaneously eliminates line current harmonics'. IEEE *Power Electronics Specialists* conference, PESC'92, Toledo, Spain, 1992,
4 KAZERAMI, M., ZIOGAS, P.D., and JOOS, G.: 'A novel active current waveshaping technique for solid-state input power factor conditioners', *IEEE Trans. Ind. Electron.*, 1991, **38**, (1), pp. 72–78
5 ZIOGAS, P.D., MORÁN, L., JOOS, G., and VINCENTI, D.: 'A refined PWM scheme for voltage and current source converters'. IEEE-IAS annual meeting, 1990, pp. 997–983
6 AKAGI, H., NABAE, A., and ATOH, S.: 'Control strategy of active power filters using multiple-voltage source PWM converters', *IEEE Trans.*, 1986, **IA-20**, (3), pp. 460–465
7 MCMURRAY, W.: 'Modulation of the chopping frequency in dc choppers and PWM inverters having current hysteresis controllers', *IEEE Trans.*, 1984, **IA-20**, (4), pp. 63–768
8 MORÁN L., GODOY, P., WALLACE, R., and DIXON, J.: 'A new current control strategy for active power filters using three PWM voltage source inverters'. IEEE PESC'93, Seattle, Washington, June 20–24, 1993